Botan, Alexandru; Favela-Rosales, Fernando; Fuchs, Patrick F.J.; Javanainen, Matti; Kanduc, Matej; Kulig, Waldemar; Lamberg, Antti; Loison, Claire; Lyubartsev, Alexander; Miettinen, Markus S.; Monticelli, Luca; Maatta, Jukka; Ollila, O.H.Samuli; Retegan, Marius; Rog, Tomasz; Santuz, Hubert; Tynkkynen, Joona

Toward Atomistic Resolution Structure of Phosphatidylcholine Headgroup and Glycerol Backbone at Different Ambient Conditions

Published in:
Journal of Physical Chemistry B

DOI:
10.1021/acs.jpcb.5b04878

Published: 01/01/2015

Document Version
Publisher's PDF, also known as Version of record

THE JOURNAL OF PHYSICAL CHEMISTRY B

Article

pubs.acs.org/JPCB

Toward Atomistic Resolution Structure of Phosphatidylcholine Headgroup and Glycerol Backbone at Different Ambient Conditions†

Alexandru Botan,[‡] Fernando Favela-Rosales,[§] Patrick F. J. Fuchs,[∥] Matti Javanainen,[⊥] Matej Kanduč,[#] Waldemar Kulig,[⊥] Antti Lamberg,[▽] Claire Loison,[‡] Alexander Lyubartsev,[○] Markus S. Miettinen,[#] Luca Monticelli,[◆] Jukka Määttä,[¶] O. H. Samuli Ollila,*[,∞] Marius Retegan,[□] Tomasz Róg,[⊥] Hubert Santuz,[▲,$,+,▽] and Joona Tynkkynen[⊥]

[‡]Institut Lumière Matière, UMR5306 Université Lyon 1-CNRS, Université de Lyon, 69622 Villeurbanne, France

[§]Departamento de Física, Centro de Investigación y de Estudios Avanzados del IPN, Apartado, Postal 14-740, Mexico City, 07000 México D.F., México

[∥]Institut Jacques Monod, UMR 7592 CNRS, Université Paris Diderot, Sorbonne, Paris Cité, F-75205 Paris, France

[⊥]Department of Physics, Tampere University of Technology, Tampere, 33101 Finland

[#]Fachbereich Physik, Freie Universität Berlin, Berlin, 14195 Germany

[▽]Department of Chemical Engineering, Kyoto University, 615-8510 Kyoto, Japan

[○]Division of Physical Chemistry, Department of Materials and Environmental Chemistry, Stockholm University, S-106 91 Stockholm, Sweden

[◆]Institut de Biologie et Chimie des Protéines (IBCP), CNRS UMR 5086, Lyon 69 367, France

[¶]Department of Chemistry, Aalto University, 00076 Aalto, Finland

[∞]Department of Neuroscience and Biomedical Engineering, Aalto University, 00076 Aalto, Finland

[□]Max Planck Institute for Chemical Energy Conversion, Stiftstr. 34-38, 45470 Mülheim an der Ruhr, Germany

[▲]INSERM, UMR_S 1134, DSIMB, Paris 75739, France

[$]Université Paris Diderot, Sorbonne Paris Cité, UMR_S 1134, Paris, France

[+]Institut National de la Transfusion Sanguine (INTS), Paris 75739, France

[▽]Laboratoire d'Excellence GR-Ex, Paris 75015, France

Supporting Information

ABSTRACT: Phospholipids are essential building blocks of biological membranes. Despite a vast amount of very accurate experimental data, the atomistic resolution structures sampled by the glycerol backbone and choline headgroup in phoshatidylcholine bilayers are not known. Atomistic resolution molecular dynamics simulations have the potential to resolve the structures, and to give an arrestingly intuitive interpretation of the experimental data, but only if the simulations reproduce the data within experimental accuracy. In the present work, we simulated phosphatidylcholine (PC) lipid bilayers with 13 different atomistic models, and compared simulations with NMR experiments in terms of the highly structurally sensitive C−H bond vector order parameters. Focusing on the glycerol backbone and choline headgroups, we showed that the order parameter comparison can be used to judge the atomistic resolution structural accuracy of the models. Accurate models, in turn, allow molecular dynamics simulations to be used as an interpretation tool that translates these NMR data into a dynamic three-dimensional representation of biomolecules in biologically relevant conditions. In addition to lipid bilayers in fully hydrated conditions, we reviewed previous experimental data for dehydrated bilayers and cholesterol-containing bilayers, and interpreted them with simulations. Although none of the existing models reached experimental accuracy, by critically comparing them we were able to distill relevant chemical information: (1) increase of choline order parameters indicates the P−N vector tilting more parallel to the membrane, and (2) cholesterol induces only minor changes to the PC (glycerol backbone) structure. This work has been done as a fully open collaboration, using nmrlipids.blogspot.fi as a communication platform; all the scientific contributions were made publicly on this blog. During the open research process, the repository holding our simulation trajectories and files (https://zenodo.org/collection/user-nmrlipids) has become the most extensive publicly available collection of molecular dynamics simulation trajectories of lipid bilayers.

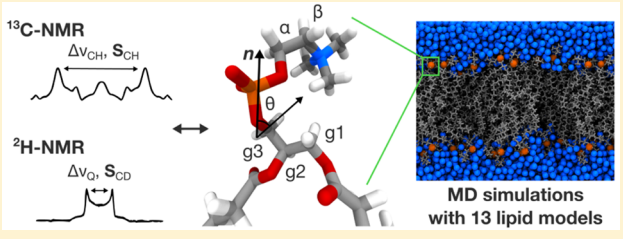

Received: May 21, 2015
Revised: October 19, 2015
Published: October 28, 2015

DOI: 10.1021/acs.jpcb.5b04878
J. Phys. Chem. B 2015, 119, 15075−15088

INTRODUCTION

Phospholipids containing various polar headgroups and acyl chains are essential building blocks of biological membranes. Lamellar phospholipid bilayer structures have been widely studied with various experimental and theoretical techniques as a simple model for cellular membranes.[1−8] Phospholipid molecules are composed of hydrophobic acyl chains connected by a glycerol backbone to a hydrophilic headgroup; see Figure 1

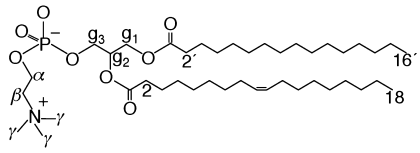

Figure 1. Chemical structure of 1-palmitoyl-2-oleoylphosphatidylcholine (POPC).

for the structure of 1-palmitoyl-2-oleoylphosphatidylcholine (POPC). The behavior of the acyl chains in a lipid bilayer is relatively well understood.[1−5,8,9] The conformations sampled by the glycerol backbone and choline in a fluid bilayer are, however, not fully resolved as even the most accurate scattering and Nuclear Magnetic Resonance (NMR) techniques give only a set of values that the structure has to fulfill, but there is no unique way to derive the actual structure from them.[9−18] Some structural details have been extracted from crystal structures, ^{1}H NMR studies, and Raman spectroscopy,[19−25] but general consensus concerning the structures sampled in the fluid state has not been reached.[9−18,24,25] Importantly, the structural parameters for the glycerol backbone are similar for various biologically relevant lipid species (phosphatidylcholine (PC), phosphatidylethanolamine (PE), and phosphatidylglycerol (PG)) in various environments,[26] and the structural parameters for the choline headgroup are similar in model membranes and real cells (mouse fibroblast L-M cell).[27] Thus, resolving the PC-lipid glycerol and choline structures would be useful for understanding a wide range of different biological membranes.

Classical atomistic molecular dynamics simulations have been widely used to study lipid bilayers.[2−7] As these models provide an atomistic resolution description of the whole lipid molecule, they have the potential to solve the glycerol backbone and headgroup structures. The experimental C−H bond order parameters (routinely compared between experiments and simulations for the acyl chains[2−6]) are also known for the glycerol backbone (g_1, g_2, and g_3) and choline (α and β) segments (see Figure 1 for definitions) and are among the main parameters used in attempts to derive lipid structures from experimental data.[10−13,15,16,18] Notably, the structures sampled in a simulation that reproduces these parameters will automatically comprise an interpretation of the experiments. In other words, such simulations can be considered as an accurate atomistic resolution description of the behavior of lipid molecules in a bilayer.

Only a few studies[28−37] have compared the glycerol backbone and choline headgroup order parameters between simulations and experiments. The main reason probably is that the existing experimental data for the glycerol backbone and choline headgroups are scattered over many publications and published in a format that is difficult to understand without some NMR expertise. In addition to the order parameters, dihedral angles for the glycerol backbone and headgroup estimated from experiments,[28,38−42] ^{31}P chemical shift anisotropy,[36] and ^{31}P−^{13}C dipolar couplings[43] have been used to assess the quality of a simulation model.

In this work, we first review the most relevant experimental data for the glycerol backbone and choline headgroup order parameters in a phosphatidylcholine lipid bilayer. Then, the available atomistic resolution lipid models are carefully compared to the experimental data. The comparison reveals that the CHARMM36,[31] GAFFlipid,[33] and MacRog[37] models have the most realistic glycerol backbone and choline structures. We also compare the glycerol backbone and choline structures between the most often used Berger-based lipid model[44] and the best performing models, to demonstrate that by using the order parameters we can distinguish the more reasonable structures from the less reasonable ones. However, none of the current models is accurate enough to properly resolve the atomistic resolution structures.

In addition to fully hydrated single component lipid bilayers, the glycerol backbone and choline order parameters have been measured under a large number of changing conditions: hydration level,[45−47] cholesterol content,[35,48] ion concentration,[49−53] temperature,[54] charged lipid content,[52,53] charged surfactant content,[55] drug molecule concentration,[30,56,57] and protein content[58,59] (listing only the publications most relevant for this work and the pioneering studies). Existence of these data allows the comparison of structural responses to varying conditions between simulations and experiments, in other words, validation of the simulation models and interpretation of the original experiments. Here we demonstrate the power of this approach in understanding the behavior of a bilayer as a function of hydration level and cholesterol content. Choline headgroup order parameters as a function of ion concentration, and their relation to the ion binding affinity, are discussed elsewhere.[60]

METHODS

Open Collaboration. This work has been done as a fully open collaboration, using the nmrlipids.blogspot.fi blog[61] as a communication platform. Our approach is inspired by the Polymath project;[62] however, there are some essential differences. We started by publishing a manuscript[63] discussing the glycerol backbone and choline structures in a Berger-based model (the most used molecular dynamics simulation model for lipid bilayers). Simultaneously, we presented an open invitation for further contributions and discussion on the blog. All the scientific contributions were made publicly through the blog. Every contributor was offered coauthorship according to the guidelines defined in the beginning of the project;[64] the acceptance of the offer was based on authors' self-assesment of their scientific contribution. These contributions are summarized in the Supporting Information.

Almost all simulation data, including input files for reproduction and trajectories for further analysis, are collected on our CERN-hosted Zenodo file repository (https://zenodo.org/collection/user-nmrlipids). Thus, in addition to the main topic of this manuscript, we present the most extensive publicly available collection of simulation trajectories for lipid bilayers, opening up numerous possiblities for different analyses with much less effort than previously required. Further information, such as scripts, figures, and manuscript text files, are available through our GitHub repository.[65]

Order Parameters from Experiments. The order parameter of a hydrocarbon C−H vector is defined as

$$S_{CH} = \frac{1}{2}\langle 3\cos^2\theta - 1\rangle \quad (1)$$

DOI: 10.1021/acs.jpcb.5b04878
J. Phys. Chem. B 2015, 119, 15075−15088

where the angle brackets denote an ensemble average over the sampled conformations, and θ is the angle between the C−H bond and the membrane normal. The absolute values of order parameters can be measured by detecting quadrupolar splitting with ^{2}H NMR[66] or by detecting dipolar splitting with ^{1}H−^{13}C NMR.[35,67−69] The measurements are based on different physical interactions, and also the connections between order parameter and quadrupolar or dipolar splitting are different. The absolute values of order parameters from the measured quadrupolar splitting $\Delta\nu_Q$ (^{2}H NMR) are calculated using the equation $|S_{CD}| = \frac{4}{3}\frac{h}{e^2qQ}\Delta\nu_Q$, where the value for the static quadrupole splitting constant is estimated from various experiments to be 170 kHz leading to a numerical relation $|S_{CD}| = 0.00784 \times \Delta\nu_Q$.[66] The absolute values of order parameters from the effective dipolar coupling d_{CH} (^{1}H−^{13}C NMR) are calculated using the equation $|S_{CH}| = 2\pi\frac{4\pi\langle r_{CH}^3\rangle}{\hbar\mu_0\gamma_H\gamma_C}d_{CH}$, where values between 20.2−22.7 kHz are used for $(2\pi\frac{4\pi\langle r_{CH}^3\rangle}{\hbar\mu_0\gamma_H\gamma_C})^{-1}$, depending on the original authors.[35,67−69] The effective dipolar coupling d_{CH} is related to the measured dipolar splitting $\Delta\nu_{CH}$ through a scaling factor that depends on the pulse sequence used in the ^{1}H−^{13}C NMR experiment.[35,67−69] It is important to note that the order parameters measured with different techniques based on different physical interactions are in good agreement with each other (see Results and Discussion), indicating very high quantitative accuracy of the measurements. For a more detailed discussion, see ref 70.

The absolute values of order parameters are accessible with both ^{2}H NMR and ^{1}H−^{13}C NMR techniques. However, only ^{1}H−^{13}C NMR techniques also allow the measurement of the sign of the order parameter.[16,67,68] The measured sign is negative for almost all the carbons discussed in this work, except for α which is positive.[16,67,68] For more detailed discussion about the determination of the sign of the order parameters, see ref 71.

For most CH_2 segments in a fluid phospholipid bilayer, the order parameters of both hydrogens are equal. However, in some cases (e.g., g_1, g_3, and C_2 carbon in the *sn*-2 chain) the two order parameters are not equal; this can be observed with both ^{2}H NMR and ^{1}H−^{13}C NMR techniques. In the present work, to avoid confusion with the dipolar and quadrupolar splittings in NMR terminology, we call the phenomenon of unequal order parameters for hydrogens attached to the same carbon *forking*. Forking has been studied in detail with ^{2}H NMR techniques by deuterating the *R* or *S* position in a CH_2 segment, and the studies show that it arises from differently sampled orientations of the two C−H bonds, not from two separate populations of lipid conformations.[26,72]

Order Parameters from Simulations. The order parameters from simulations were calculated directly using the definition of eq 1. For the united atom models, the hydrogen positions were generated post-simulationally from the positions of the heavy atoms and the known hydrocarbon geometries. The statistical error was estimated on the basis of the assumption that different lipids are statistically independent entities, which should be the case in fluid phase: The time average of a given order parameter was first calculated separately for each lipid, then the standard error of the mean over the time averages was taken as the error bar for this order parameter.

It has been pointed out that the sampling of individual dihedral angles might be very slow compared to the typical (100 ns) simulation time scales.[73] After 200 ns, however, even the slowest rotational correlation function of a C−H bond (g_1) reaches a plateau (S_{CH}^2) in the Berger-POPC-07 model,[74] and notably, the dynamics of this segment have been shown to be significantly slower in simulations than in experiments.[75] In practice, due to averaging over different lipid molecules, less than 200 ns of simulation data should be enough for the order parameter calculation; if the sampling within typical simulation times is not enough for the convergence of the order parameters, then the simulation model in question has unphysically slow dynamics.

Simulated Systems. All simulations are run with a standard setup for a planar lipid bilayer in zero tension and constant temperature with periodic boundary conditions in all directions by using the GROMACS software package[76] (version numbers 4.5.X−4.6.X), LAMMPS,[77] MDynaMix,[78] or NAMD.[79] The number of molecules, simulation temperatures, and the length of simulations of all the simulated systems are listed in Tables 1, 2 and 3. Full simulation details are given in the Supporting Information (SI) or in the original publications in case the data is used previously therein. All simulation parameters were set as close to the original parametrization works as possible. Additionally, the files related to the simulations and the resulting trajectories are publicly available for almost all systems in the Zenodo collection https://zenodo.org/collection/user-nmrlipids. The references pointing to simulation details and files are also listed in Tables 1−3.

RESULTS AND DISCUSSION

Full Hydration: Experimental Order Parameters for the Glycerol Backbone and Headgroup. The specific deuteration of α, β, and g_3 segments of DPPC has been successful, allowing the absolute values of the order parameters for these segments to be measured by ^{2}H NMR.[48−50,54] In addition, the absolute values of order parameters for all glycerol backbone and choline headgroup segments in egg yolk lecithin,[67] DMPC,[16,68,69] DOPC,[141] and POPC[35,141] have been measured with several different implementations of ^{1}H−^{13}C NMR experiments. Furthermore, for some systems the signs of the order parameters have been measured with ^{1}H−^{13}C NMR techniques.[16,67,68] The experimental values of the glycerol backbone and choline order parameters from various publications,[35,50,54,68,69] with the signs measured in refs 16, 67, and 68, are shown in Figure 2.

In general there is a good agreement between the order parameters measured with different experimental NMR techniques. Almost all the reported values are within a variation of ±0.02, which is also the error estimate given by Gross et al.[68] for all fully hydrated PC bilayers, regardless of variation in their acyl chain composition and temperature. Exceptions are the somewhat lower order parameters reported from some measurements using ^{1}H−^{13}C NMR.[16,67,141] In these experiments, however, either the reported error bars are relatively large,[16,67] or the spectral resolution is quite low and numerical line shape simulations have not been used in the analysis.[141] As it, therefore, is highly likely that the reported lower order parameters are due to lower experimental accuracy, we exclude them from the present discussion; for more details, see ref 70. Motivated by the high experimental reproducibility, we have highlighted in Figure 2 subjective sweet spots (light blue areas spanning 0.04 units around the average of the extremal experimental values), within which we expect the calculated values of the order parameters of a well-performing force field to fall.

In addition to the numerical values, forking (see Order Parameters from Experiments section) is an important feature of the order parameters. In contrast to the lack of forking in the

DOI: 10.1021/acs.jpcb.5b04878
J. Phys. Chem. B 2015, 119, 15075−15088

Table 1. Fully Hydrated Single Component Lipid Bilayer Systems Simulated for Figure 2: 1,2-Dimyristoyl-*sn*-glycero-3-phosphocholine (DMPC), Dilauroylphosphatidylcholine (DLPC), Dipalmitoylphosphatidylcholine (DPPC), and 1-Palmitoyl-2-oleoylphosphatidylcholine (POPC)[a]

force field	lipid	N_l[b]	N_w[c]	T[d] (K)	t_{sim}[e] (ns)	t_{anal}[f] (ns)	files[g]	details[h]
Berger-DMPC-04[80]	DMPC	128	5097	323	130	100	81*	82
Berger-DPPC-98[83]	DPPC	72	2864	323	60	30	84*	SI
Berger-POPC-07[74]	POPC	128	7290	298	270	240	85*	75
CHARMM36[31]	DPPC	72	2189	323	30	25	86*	SI
CHARMM36[31]	DPPC	72	2189	323	130			31[i]
CHARMM36[31]	POPC	72	2242	303	30	20	87*	SI
CHARMM36[31]	POPC	128	5120	303	200	100	88*	SI
MacRog[89]	POPC	288	12 600	310	100	80	90*	SI
MacRog[89]	POPC	128	6400	310	400	200	91*	SI
MacRog[89]	POPC	288	14 400	310	90	40	92*	SI
GAFFlipid[33]	DPPC	72	2197	323	90	50	93*	SI
GAFFlipid[33]	DPPC	72	2167	323	250	250		33[j]
GAFFlipid[33]	POPC	126	3948	303	137	32	94*	SI
Lipid14[95]	POPC	72	2234	303	100	50	96*	SI
Poger[97]	DPPC	128	5841	323	2 × 100	2 × 50	98, 99*	SI
Slipids[100]	DPPC	128	3840	323	150	100	101*	SI
Slipids[102]	POPC	128	5120	303	200	150	103*	SI
Kukol[104]	POPC	512	20 564	298	50	30	105*	SI
Chiu[106]	POPC	128	3552	298	56	50	107*	SI
Högberg08[29]	DMPC	98	3840	303	75	50	108*	29
Högberg08[109]	POPC	128	3840	303	100	80	110*	109
Ulmschneiders[111]	POPC	128	3328	310	100	50	112*	SI
Tjörnhammar14[113]	DPPC	144	7056	323	200	100	114*	113
Botan-CHARMM36-UA[115]	DLPC	128	3840	323	30	20	116	SI
Lee-CHARMM36-UA[117]	DPPC	72	2189	323	70	50	118*	SI

[a]The **bolded** systems were used also for Figure 3. [b]Number of lipid molecules. [c]Number of water molecules. [d]Temperature. [e]Total simulation time. [f]Time used for analysis. [g]Reference link for the downloadable simulation files; the data sets marked with an asterisk also include a part of the trajectory. [h]Reference for the full simulation details. The original publication is cited if simulation data from previously published work has been directly used; for other systems the simulation details are given in the Supporting Information. [i]Magnitudes from Figure S4 of Klauda et al.;[31] signs matched to our simulations. [j]Magnitudes from Figure 9 of Dickson et al.;[33] signs matched to our simulations.

Table 2. Simulated Single Component Lipid Bilayers with Varying Hydration Levels[a]

force field	lipid	n[b] (w/l)	N_l[c]	N_w[d]	T[e] (K)	t_{sim}[f] (ns)	t_{anal}[g] (ns)	files[h]	details[i]
Berger-POPC-07[74]	POPC	57	128	7290	298	270	240	85*	SI
	POPC	7	128	896	298	60	50	119*	SI
Berger-DLPC-13[120]	DLPC	28	72	2016	300	80	60	121*	120
	DLPC	24	72	1728	300	80	60	122*	120
	DLPC	20	72	1440	300	80	60	123*	120
	DLPC	16	72	1152	300	80	60	124*	120
	DLPC	12	72	864	300	80	60	125*	120
	DLPC	8	72	576	300	80	60	126*	120
	DLPC	4	72	288	300	80	60	127*	120
CHARMM36[31]	POPC	40	128	5120	303	150	100	88*	SI
	POPC	31	72	2242	303	30	20	87*	SI
	POPC	15	72	1080	303	59	40	128*	SI
	POPC	7	72	504	303	60	20	129*	SI
MacRog[89]	POPC	50	288	14 400	310	90	40	92*	SI
	POPC	44	288	12 600	310	100	80	90*	SI
	POPC	25	288	7200	310	100	50	92*	SI
	POPC	20	288	5760	310	100	50	92*	SI
	POPC	15	288	4320	310	100	50	92*	SI
	POPC	10	288	2880	310	100	50	92*	SI
	POPC	5	288	1440	310	100	50	92*	SI
GAFFlipid[33]	POPC	31	126	3948	303	137	32	94*	SI
	POPC	7	126	896	303	130	40	130*	SI

[a]The simulation file data sets marked with an asterisk also include part of the trajectory. [b]Water/lipid molar ratio. [c]The number of lipid molecules. [d]The number of water molecules. [e]Simulation temperature. [f]The total simulation time. [g]Time frames used in the analysis. [h]Reference link for the downloadable simulation files. [i]Reference for the full simulation details.

DOI: 10.1021/acs.jpcb.5b04878
J. Phys. Chem. B 2015, 119, 15075−15088

Table 3. Simulated Lipid Bilayers Containing Cholesterol[a]

force field	lipid	N_l[b]	N_{chol}[c]	C_{CHOL}[d]	N_w[e]	T[f] (K)	t_{sim}[g] (ns)	t_{anal}[h] (ns)	files[i]	details[j]
Berger-POPC-07[74]/Höltje-CHOL-13[35,131]	POPC	128	0	0%	7290	298	270	240	85*	75
	POPC	120	8	6%	7290	298	100	80	132*	35
	POPC	110	18	14%	8481	298	100	80	133*	35
	POPC	84	44	34%	6794	298	100	80	134*	35
	POPC	64	64	50%	10 314	298	100	80	135*	35
	POPC	50	78	61%	5782	298	100	80	136*	35
CHARMM36[31,137]	POPC	128	0	0%	5120	303	150	100	88*	SI
	POPC	512	0	0%	23 943	298	170	100	138*	SI
	POPC	460	52	10%	23 569	298	170	100	138*	SI
	POPC	436	76	15%	23 331	298	170	100	138*	SI
	POPC	100	24	19%	4960	303	200	100	139*	SI
	POPC	410	102	20%	20 972	298	170	100	138*	SI
	POPC	384	128	25%	22 327	298	170	100	138*	SI
	POPC	332	180	35%	21 340	298	170	100	138*	SI
	POPC	256	256	50%	20 334	298	170	100	138*	SI
	POPC	80	80	50%	4496	303	200	100	140*	SI
MacRog[89]	POPC	128	0	0%	6400	310	400	200	91*	SI
	POPC	114	14	11%	6400	310	400	200	91*	SI
	POPC	72	56	44%	6400	310	400	200	91*	SI
	POPC	64	64	50%	6400	310	400	200	91*	SI
	POPC	56	72	56%	6400	310	400	200	91*	SI

[a]The simulation file data sets marked with an asterisk also include part of the trajectory. [b]The number of lipid molecules. [c]The number of cholesterol molecules. [d]Cholesterol concentration (mol %). [e]The number of water molecules. [f]Simulation temperature. [g]The total simulation time. [h]Time frames used in the analysis. [i]Reference link for the downloadable simulation files. [j]Reference for the full simulation details.

choline segments α and β, both CH_2 segments of the glycerol backbone fork. In the g_3 segment, forking is small (≈0.02), and some experiments only report the larger or the average value.[35,50] However, forking is significant for the g_1 segment, whose lower order parameter is close to zero, and the larger one has an absolute value of approximately 0.13−0.15. Forking was studied in detail by Gally et al.,[26] who used *E. coli* to stereospecifically deuterate the different hydrogens attached to the g_1 or g_3 groups in PE lipids, and measured the order parameters from the lipid extract. This experiment gave the lower order parameter when deuterium was in the *S* position of g_1 or *R* position for g_3. Since the glycerol backbone order parameters are very similar irrespective of the headgroup chemistry (PC, PE, or PG) or lipid environment,[26] it is reasonable to assume that the stereospecifity measured for the PE lipids holds also for the PC lipids.

The most detailed experimentally available order parameter information for the glycerol backbone and choline segments of POPC bilayer is collected by taking the absolute values from ref 35, the signs from refs 16, 67, and 68, and the stereospecific labeling from ref 26, and is shown in Figure 3.

Full Hydration: Comparison between Simulation Models and Experiments. The order parameters of the glycerol backbone and headgroup calculated from different force fields for various lipids have been previously compared to those from experiments.[28−37] The general conclusion from these studies seems to be that the CHARMM-based,[29,31] GAFFlipid,[33] and MacRog[37] force fields performs better for the glycerol backbone and headgroup structures than the GROMOS-based models.[30,32,34,35] However, none of the studies exploits the full potential of the available experimental data discussed in the previous section, i.e. the quantitative accuracy, known signs, and stereospecific labeling of the experimental order parameters.

To get a general idea of the quality of the glycerol backbone and choline headgroup structures in different models, we calculated the order parameters for these parts from 13 different lipid models (Table 1) and plotted the results together with experimental values in Figure 2. Two criteria were used to judge the quality of the model. (1) There must not be significant forking in the α and β carbons, there must be only moderate forking in the g_3 carbons, and there must be significant forking in the g_1 carbon. (2) The magnitude should be preferably inside the subjective sweet spots determined from experiments (blue shaded regions in Figure 2). The results for each force field with respect to the above criteria are summarized in Figure 4.

None of the studied force fields fulfills these criteria completely; however, CHARMM36 is close. This is not surprising since the dihedral potentials in this model are tuned against experiments to better reproduce these order parameters.[31] The next models in the list are CHARMM36-UA[115,117] and Högberg08,[29] which is also not surprising since these models are using the CHARMM bonded potentials for glycerol backbone and choline. The fourth and the fifth models in the list, MacRog[37] and GAFFlipid,[33] have independently determined dihedral potentials. All the models based on GROMOS potentials and Slipids perform less well. In the following sections we subject CHARMM36, MacRog, GAFFlipid, and Berger-POPC-07 to a more careful comparison including the stereospecific labeling (Figure 3), atomistic level structure, and responses to dehydration and cholesterol content. These models are selected for more detailed study since they are the best representatives of different dihedral potential parametrization techniques (CHARMM36, MacRog, GAFFlipid), and the Berger-based models are the most used lipid models in the literature.

Full Hydration: Atomistic Resolution Structures in Different Models. The results in the previous section revealed significant differences of the glycerol backbone and choline headgroup order parameters between different molecular dynamics simulation models. However, it is not straightforward to conclude which kind of structural differences (if any) between the models the results indicate, because the mapping from the

DOI: 10.1021/acs.jpcb.5b04878
J. Phys. Chem. B 2015, 119, 15075−15088

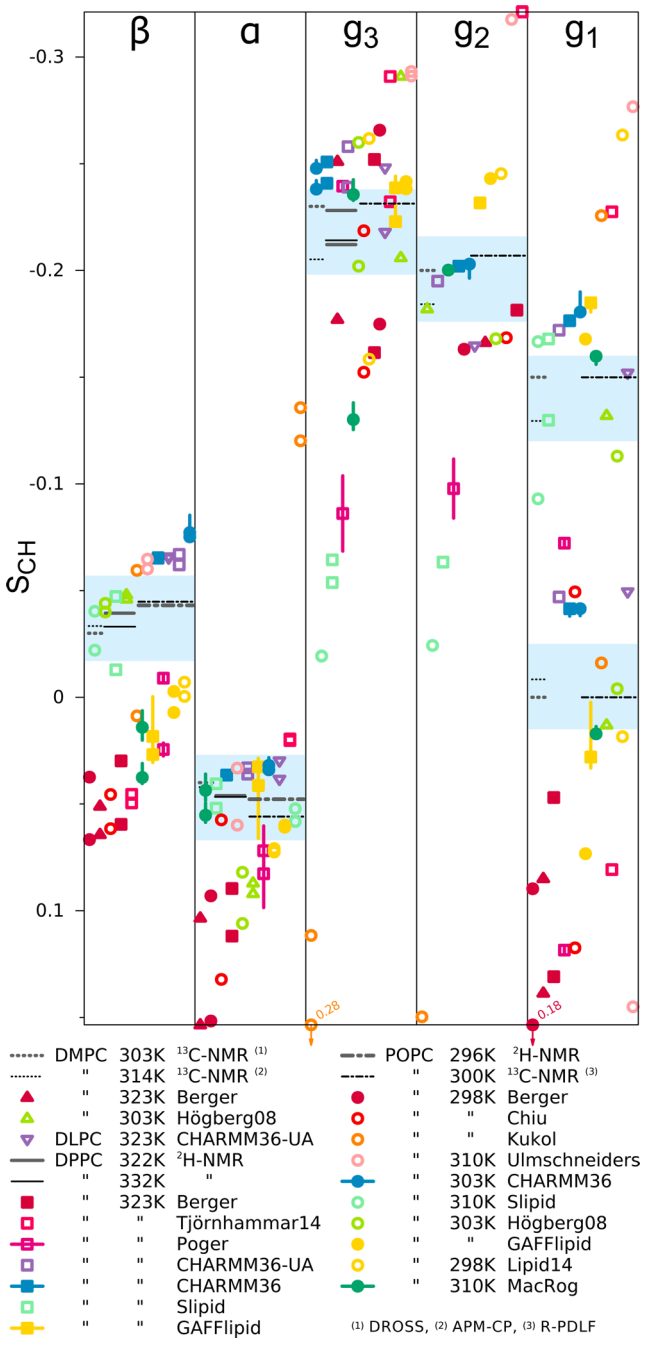

Figure 2. Order parameters from simulations listed in Table 1 and experiments for glycerol and choline groups. The experimental values were taken from the following publications: DMPC 303 K from ref 68, DMPC 314 K from ref 69, DPPC 322 K from ref 54, DPPC 323 K from ref 50, POPC 296 K from ref 45, and POPC 300 K from ref 35. The vertical bars shown for some of the computational values are not error bars, but demonstrate that for these systems we had at least two data sets (see Table 1); the ends of the bars mark the extreme values from the sets, and the dot marks their measurement-time-weighted average. An interactive version of this figure is available at https://plot.ly/~HubertSantuz/72/lipid-force-fieldcomparison/.

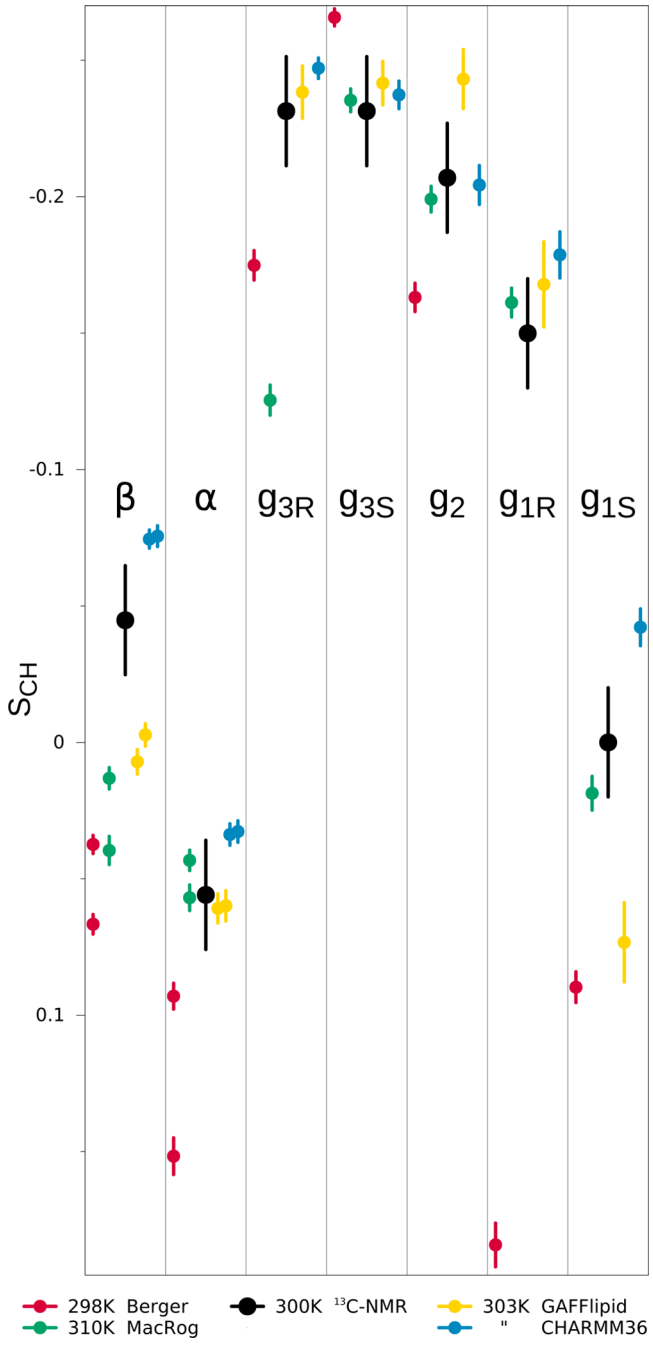

Figure 3. Order parameters for POPC glycerol and choline groups from simulations with Berger-POPC-07, MacRog, GAFFlipid, and CHARMM36 force fields (the **bolded** systems in Table 1) together with experimental values. The error bars of simulation data are standard errors of mean (see Methods section for details). The magnitudes for experimental order parameters are taken from Ferreira et al.,[35] the signs are based on the measurements by Hong et al.[16,67] and Gross et al.,[68] and the *R*/*S* labeling is based on the measurements by Gally et al.[26]

order parameters to the structure is not unique. In this section we demonstrate that (1) the differences in order parameters indicate significantly different structural sampling, which is strongly correlated with the dihedral angles of the related bonds, and that (2) the comparison between experimental and simulated order parameters can be used to exclude nonrealistic structural sampling in molecular dynamics simulations. The demonstration is done for the dihedral angles defined by the $g_3-g_2-g_1-O(sn\text{-}1)$ segments in the glycerol backbone and the N-β-α-O segments in the headgroup. These dihedrals were chosen for demonstration, because significant differences between the models are observed around these segments in Figure 3. We note that performing a similar comparison through all the dihedrals in all the 13 models would probably give highly useful information on how to improve

DOI: 10.1021/acs.jpcb.5b04878
J. Phys. Chem. B 2015, 119, 15075−15088

	β	α	g_3	g_2	g_1	Σ
CHARMM 36	M		M		M	3
CHARMM 36-UA	M	F	M	M	M F	6
Högberg08		M F	M **F**	M	F	8
MacRog	**M** F	F	**M F**		M F	8
GAFFlipid	M F	F	M F	M	**M F**	9
Lipid14	M F	M	M **F**	M	**M F**	11
Chiu	**M** F	**M F**	M F	M	**M** F	11
Ulmschneiders	M	F	M F	**M**	**M F**	12
Slipid	**F**	F	**M** F	**M**	**M F**	13
Poger	**M F**	M F	**M F**	**M**	**M** F	13
Tjörnhammar14	**M**	M	M **F**	**M**	**M F**	15
Berger	**M** F	**M F**	M **F**	M	**M F**	15
Kukol	M **F**	**M** F	**M F**	**M**	M F	16

Figure 4. Rough subjective ranking of force fields based on Figure 2. Here "M" indicates a magnitude problem, "F" a forking problem; letter size increases with problem severity. Color scheme: "within experimental error" (dark green), "almost within experimental error" (light green), "clear deviation from experiments" (light red), and "major deviation from experiments" (dark red). The Σ-column shows the total deviation of the force field, when individual carbons are given weights of 0 (matches experiment), 1, 2, and 4 (major deviation). For full details of the assessment, see Supporting Information.

the accuracy of the models, yet this is beyond the scope of the current report.

The dihedral angle distributions for the $g_3-g_2-g_1-O(sn\text{-}1)$ dihedral calculated from different models are shown in Figure 5. The distribution is qualitatively different for the Berger-POPC-07 model, showing a maximum in the gauche$^+$-conformation (60°) compared to all the other models showing a maximum in the anti conformation (180°). The distributions in all the other models have the same general features, with the main difference being that the fraction of configurations in the gauche$^-$-conformation (−60°) is zero for the MacRog, detectable for the CHARMM36 and equally large to the gauche$^+$ fraction in GAFFlipid. From the results we conclude that most likely the wrongly sampled dihedral angle for the g_2-g_1 bond explains the significant discrepancy to the experimental order parameters for the g_1 segment in the Berger-POPC-07 model (Figure 3).

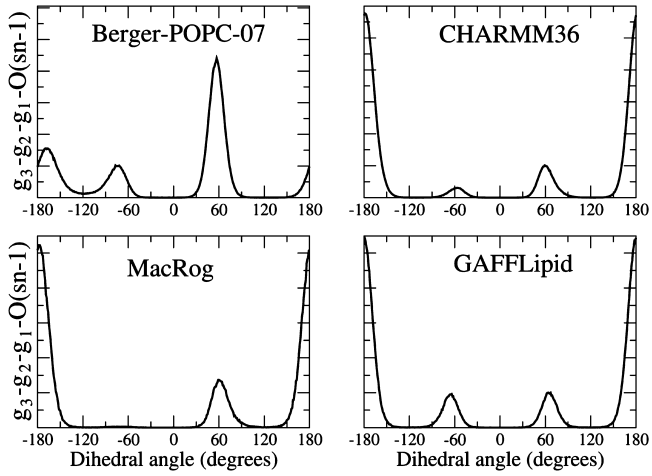

Figure 5. Dihedral angle distributions for $g_3-g_2-g_1-O(sn\text{-}1)$ dihedral from different models (POPC bilayer in full hydration).

In conclusion, models preferring the anti conformation for this dihedral give more realistic order parameters; this is in agreement with previous crystal structure and ^{1}H NMR studies.[19−21,23−25]

The dihedral angle distribution for the N-β-α-O dihedral calculated from the same four models is shown in Figure 6.

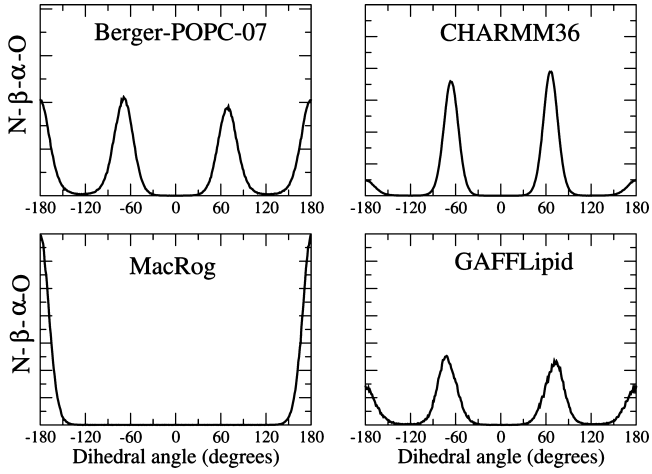

Figure 6. Dihedral angle distributions for N-β-α-O dihedral from different models (POPC bilayer in full hydration).

Also for this dihedral there are significant differences in the gauche−anti fractions. The gauche conformations are dominant in CHARMM36, only anti conformations are present in MacRog, while in Berger-POPC-07 and GAFFlipid the gauche and anti conformations have equal probabilities. On the other hand, comparison of α and β order parameters in Figure 3 reveals that for these carbons the CHARMM36 is closest to the experimental results, and it is also the only model that has the correct sign (negative) for the β order parameter. This result is again in agreement with previous crystal structure, ^{1}H NMR, and Raman spectroscopy studies,[19−22] which suggest that this dihedral is in the gauche conformation in the absence of ions.

These examples show that the glycerol backbone and headgroup order parameters reflect the atomistic resolution structure and that the comparison with experiments allows the assessment of the quality of the suggested structure. We were able to pinpoint specific problems in the structures in different models and suggest potential improvement strategies. If an improved

DOI: 10.1021/acs.jpcb.5b04878
J. Phys. Chem. B 2015, 119, 15075−15088

atomistic molecular dynamics simulation model would reproduce the order parameters and other experimental observables (like ^{31}P chemical shift anisotropy[36] and ^{31}P−^{13}C dipolar couplings[43]) within experimental accuracy, it would give an interpretation for the atomistic resolution structure of the glycerol backbone and choline.[10−13,15,16,18] The research along these lines is left, however, for future studies.

Response to Dehydration and Cholesterol Content. In addition to pure phosphatidylcholine bilayers at full hydration, the choline headgroup order parameters have been measured under various different conditions.[30,32,35,45−51,54,55] Also, the order parameters for the glycerol backbone have been measured with ^{1}H−^{13}C NMR in dehydrated conditions,[47] and as a function of anesthetics[30] and glycolipids[32] for DMPC, and as a function of cholesterol concentration for POPC.[35] Due to the high resolution in the NMR (especially ^{2}H NMR) experiments, even very small order parameter changes resulting from the varying conditions can be measured (see ref 70 for more discussion), but as already discussed above, it is not simple to deduce the structural changes from order parameter changes.[15,18] However, comparison of the order parameters between simulations and experiments in different conditions can be used to assess the quality of the force field in different situations, and, if the quality is good, to interpret the structural changes in experiments. Here we exemplify such a comparison for a lipid bilayer under low hydration levels and when varying amounts of cholesterol are included in the bilayer. The interaction between ions and a phosphatidylcholine bilayer will be discussed in a separate study.[60]

Phospholipid Bilayer with Low Hydration Level. Figure 7 shows the published[45−47] experimental order parameters for the glycerol backbone and choline as a function of hydration level. Despite slight differences in temperature and acyl chain composition, the three independently reported data sets for the choline (β and α) segments agree well with each other: Both order parameters increase with decreasing hydration level. The glycerol backbone order parameters (g_3, g_2, g_1), in contrast, have been observed[47] to slightly decrease with dehydration. Note that the original experiments[45−47] measured only absolute values, but here we included the signs measured in separate studies.[16,67,68] Consequently, the negative β order parameter actually increases with dehydration as its absolute value decreases.[45−47]

Lipid bilayer dehydration has been studied also with molecular dynamics simulations,[142−147] typically motivated by the discussion concerning the origin of the "hydration repulsion".[148−150] Only one[142] of these studies, however, compared their simulation model to the experimental choline and glycerol backbone order parameters. Figure 7 shows these order parameters as a function of hydration level for the CHARMM36, MacRog, and GAFFlipid models (having the most realistic atomistic resolution structures) and a Berger-based model (which is the most used lipid model); note that the simulation results have been vertically shifted to ease the comparison with experimental response to dehydration. Despite some fluctuations, the increase of the choline (β and α) order parameters is seen in all four models. The response of the choline order parameters to dehydration can, therefore, be interpreted to qualitatively agree with experiments. The situation is significantly more complicated for the glycerol backbone: None of the four models produced the experimentally seen trends in all the (g_3, g_2, g_1) segments.

The qualitative agreement of the α and β order parameters with experiments in all four simulation models (Figure 7) indicates that, despite the unrealistic structures at full hydration (Figures 2 and 4), the structural response of the choline

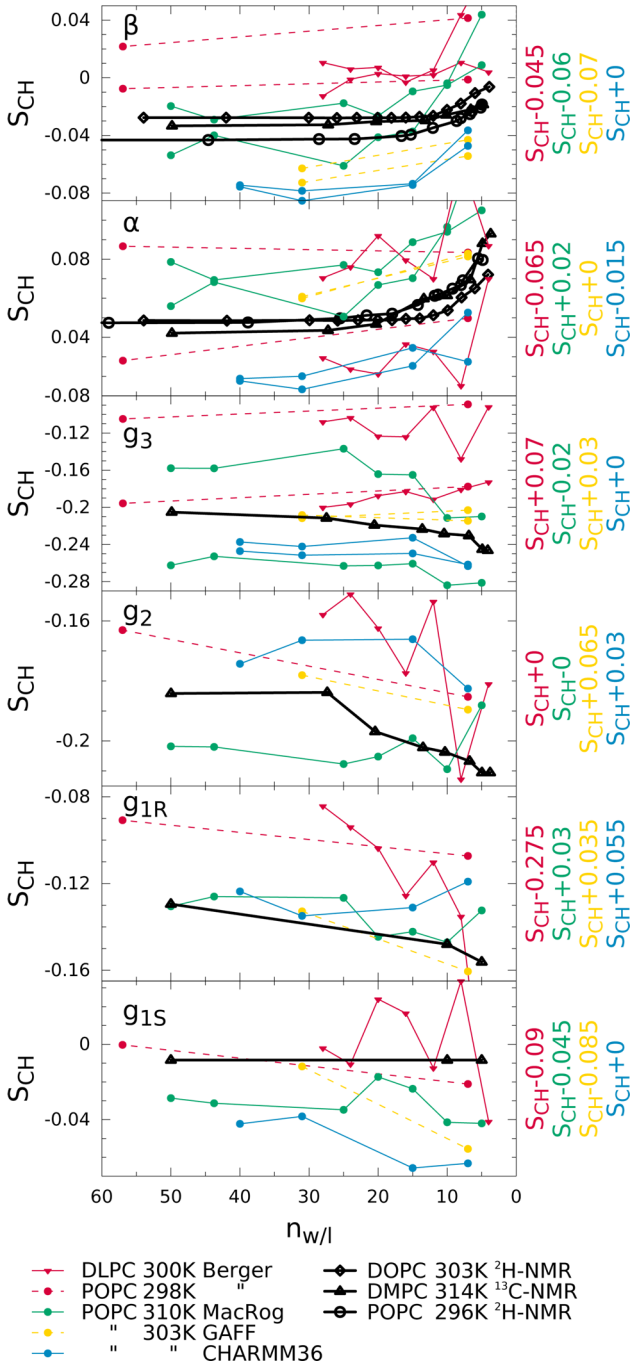

Figure 7. Effect of dehydration on glycerol and choline order parameters in experiments. The magnitudes of order parameters are measured for DMPC (^{1}H−^{13}C NMR) at 314 K,[47] for POPC (^{2}H NMR) at 296 K,[45] and for DOPC (^{2}H NMR) at 303 K.[46] The signs are based on the measurements by Hong et al.[16,67] and Gross et al.[68] Note that to elucidate the relative change as a function of hydration level, the simulation results were vertically shifted; the shift magnitudes for each of the force fields are listed (S_{CH} + shift) in the *y*-label.

headgroup to dehydration is somewhat realistic. A likely explanation is that as the interlamellar space shrinks with dehydration, the whole choline group orients more parallel to the membrane. Indeed, upon dehydration the angle between P−N (phoshate phosphorus to choline nitrogen) vector and membrane normal increases for all four models (Figure 8). However, the amount of increase depends on the model. Especially, the DLPC simulations with Berger model predict a significantly stronger

DOI: 10.1021/acs.jpcb.5b04878
J. Phys. Chem. B 2015, 119, 15075−15088

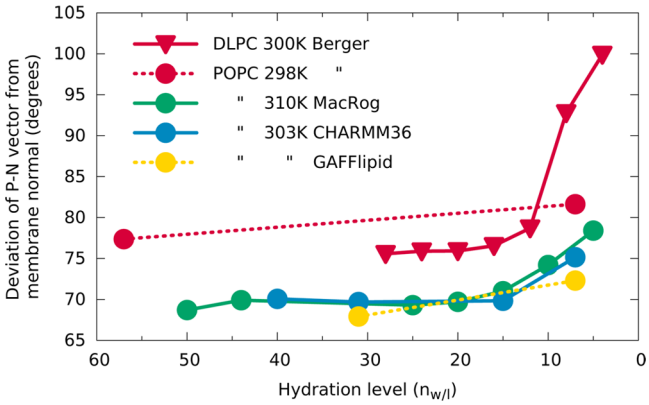

Figure 8. Average angle between membrane normal and P−N vector as a function of hydration level calculated from different simulations.

P−N vector tilt than the other models. The Berger model also has generally larger P−N vector angles, and its choline order parameters are more off from experiments than the other three models (Figure 3). Thus, the relatively modest tilting with dehydration predicted by MacRog, CHARMM36, and GAFFlipid is probably more realistic.

It must be stressed that in the models incapable of reproducing the experimental order parameters the free energy landscape is not correct. Thus, even though the order parameter response to dehydration is qualitatively correct, the energetic response is likely to be incorrect. This may have some influence on dehydration energetic calculations made using the Berger model.[145,147]

The response of the glycerol backbone seems to be more subtle than that of the choline headgroup; none of the four models reproduced the experimental trends upon dehydration with enough accuracy to invite a structural interpretation.

Cholesterol-Containing Phospholipid Bilayer. As cholesterol is abundant in biological membranes and has been suggested to be an important player, for example, in domain formation,[151,152] phospholipid−cholesterol interactions have been extensively studied with theoretical[153−156] and experimental[8,35,48,157] methods. It is widely agreed that cholesterol orders lipid acyl tails and thus decreases the area per molecule (condensing effect), but its influence on the lipid headgroup and glycerol backbone remains debated.[151−153] It has been suggested, for example, that the surrounding phospholipids shield cholesterol from exposure to water by reorienting their headgroups ("umbrella model")[153] or that cholesterol acts as a spacer between the headgroups to increase their entropy and dynamics ("superlattice model").[152] Molecular dynamics simulations have supported both the umbrella[156] as well as the superlattice[154] model, in addition to suggesting specific interactions of cholesterol with the glycerol backbone.[155] In these studies[154−156] the responses of the glycerol backbone and choline headgroup to increasing cholesterol content were not, however, compared to experiments.

Figure 9 shows the responses of the choline headgroup (β and α) order parameters of POPC (measured by ^{1}H−^{13}C NMR[35]) and DPPC (^{2}H NMR[48]) to increasing cholesterol content. Again, the two independent data sets agree very well: Only very modest (ΔS_{CH} < 0.03) changes occur in the choline order parameters as cholesterol content increases from 0 to 60%. The extreme sensitivity of the high resolution ^{2}H NMR experiments is beautifully demonstrated by the measurable[48] (but barely visible on the scale used in Figure 9) cholesterol-induced forking of the α order parameter.

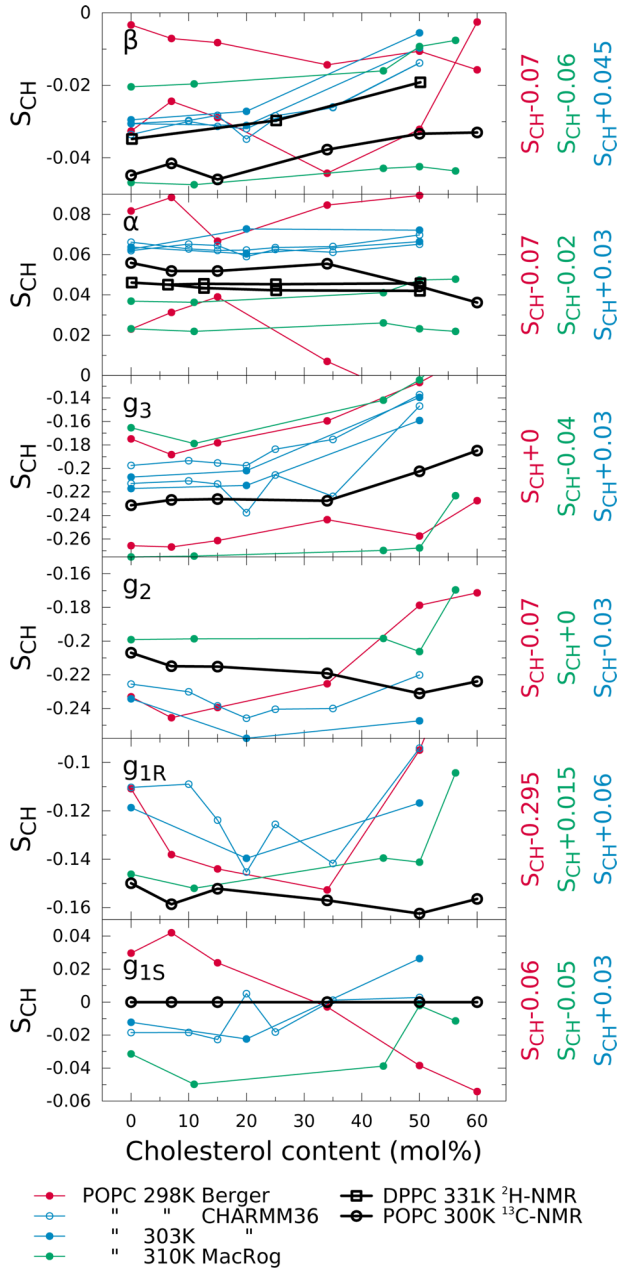

Figure 9. Effect of cholesterol content on the glycerol backbone and choline order parameters in experiments[35,48] and simulations with the Berger-POPC-07/Höltje-CHOL-13, CHARMM36, and MacRog force fields. The signs in the experimental values are based on the measurements by Hong et al.[16,67] and Gross et al.[68] In order to elucidate the relative change as a function of cholesterol content, the simulation results were vertically shifted; the shift magnitudes for each of the force fields are listed (S_{CH} + shift) in the *y*-label.

We note that the modest (ΔS_{CH} < 0.02 for g_1; <0.04 for g_2, g_3; see Figure 9) effects of cholesterol on the glycerol backbone order parameters of POPC measured by ^{1}H−^{13}C NMR[35] agree well with the results for phosphatidylethanolamine (PE) measured by ^{2}H NMR.[158] This further supports the ideas that the glycerol backbone structural behavior is independent of the headgroup composition[26] and that the headgroup structure is largely independent of the acyl chain region content unless charges are present.[27]

In addition to the experimental data, Figure 9 shows our results for the CHARMM36 and MacRog force fields and the previously

DOI: 10.1021/acs.jpcb.5b04878
J. Phys. Chem. B 2015, 119, 15075−15088

published[35] Berger-POPC-07/Höltje-CHOL-13 results. Note that the simulation data are shifted vertically to ease comparison with experimental responses. As previously pointed out,[35] the Berger-based model seriously exaggerates the effect of cholesterol on the phospholipid glycerol backbone and choline headgroup. In comparison, the choline and glycerol backbone responses of CHARMM36 and MacRog are in better qualitative agreement with experiments. Therefore, to resolve the nature of cholesterol-induced structural changes, we calculated from CHARMM36 the glycerol backbone orientation and dihedral angle distributions at various cholesterol contents (Supporting Information). The only detectable changes are the small decrease of gauche(−) and increase of gauche(+) probability of the $g_3-g_2-g_1-O(sn\text{-}1)$ dihedral and slight (less than 5°) change in the glycerol backbone orientation. In conclusion, our results suggest that the significant effects of cholesterol on lipid conformations observed in simulations[154−156] are overestimated by the computational models used; cholesterol only induces very small structural changes in the glycerol backbone.

Finally, it is important to note that the CHARMM36 force field parameters (glycerol backbone dihedral potentials) have been tuned to reproduce the experimental order parameters at full hydration.[31] This approach introduces a risk of overfitting, which would manifest itself as wrong responses to changing conditions. Interestingly, according to our results, tuning did not lead to overfitting problems as far as dehydration or cholesterol content is considered.

CONCLUSIONS

The atomistic resolution structures sampled by the glycerol backbone and choline headgroup in phoshatidylcholine bilayers are not known despite vast amounts of accurate experimental data. An atomistic resolution molecular dynamics simulation model that would reproduce the experimental data would automatically resolve the structures, thus giving an unprecedently detailed interpretation of the experimental data. In this work we have collected and reviewed the experimental C−H bond vector order parameters available in the literature. These accurate experimental data are then compared to 13 different atomistic resolution simulation models for a fully hydrated lipid bilayer system, followed by bilayers dehydrated to different extents, and finally bilayers containing various amounts of cholesterol. We are led to the following four main conclusions. (1) The C−H bond order parameters measured with different NMR techniques are consistent. By combining the experimental results from various sources, we concluded that the order parameters for each C−H bond are known with a quantitative accuracy of ±0.02. (2) Comparison of order parameters between experiments and different atomistic resolution models together with structural analysis showed that the order parameters can be used to judge the structural accuracy of a model. Thus, the combination of atomistic resolution molecular dynamics simulations and NMR experiments can be used to resolve the atomistic resolution structures of biomolecules in biologically relevant conditions. This approach can be extended from lipids to, for example, membrane proteins. (3) The review of previous experimental results revealed that when a bilayer is dehydrated the choline order parameters increase. Our simulations suggested that this can be explained by the P−N vector tilting more parallel to the membrane. This strongly supports and complements the idea that charge-induced choline tilting can be measured using order parameter changes.[55,60] (4) Only modest changes of glycerol backbone and choline order parameters are observed experimentally with increasing cholesterol content. When interpreted using the computational lipid model that we found to have the most realistic response to cholesterol, this observation means that cholesterol induces only minor changes in the $g_3-g_2-g_1-O(sn\text{-}1)$ dihedral of the glycerol backbone; in other words, there is no major conformational change of the lipid. Besides these four main conclusions, we note that we have created the most extensive publicly available collection of molecular dynamics simulation trajectories of lipid bilayers (https://zenodo.org/collection/user-nmrlipids). The mere existence of this collection opens up numerous possibilities for unforeseen analyses, such as data mining, and rapid testing of ideas with much less computational effort than previously required.

In general, we conclude that, in order to fully utilize the potential of atomistic-resolution classical molecular dynamics simulations in the structural interpretation of high resolution NMR data[159] for lipid bilayers, one must improve the phoshatidylcholine glycerol backbone and choline headgroup parameters of the existing force fields.

This work has been done as a fully open collaboration, using nmrlipids.blogspot.fi as the communication platform. All the scientific contributions have been communicated publicly through this blog.[61]

ASSOCIATED CONTENT

Supporting Information

The Supporting Information is available free of charge on the ACS Publications website at DOI: 10.1021/acs.jpcb.5b04878.

Simulation and analysis details, two figures, and author contributions (PDF)

AUTHOR INFORMATION

Corresponding Author

*E-mail: samuli.ollila@aalto.fi.

Notes

The authors declare no competing financial interest.

[†]Publication about results presented in the NMRlipids project.

This article contains links to data sources hosted outside of the ACS journals platform. As a result, readers should be aware that ACS is not able to confirm the long-term accessibility of these external data sources.

ACKNOWLEDGMENTS

We acknowledge all the discussion participants at nmrlipids.blogspot.fi. A.B. and C.L. acknowledge financial support from the French National Research Agency (ANR: Biolubrication by phospholipid membranes, Biolub2012) and computing time allocation from Pôle Scientifique de Modélisation Numérique from the ENS Lyon (PSMN), and Centre Informatique National de l'Enseignement Supérieur (CINES, Montpelier, France) (Project c2015096850). F.F.-R. acknowledges CONACYT and DGAPA UNAM IG100513 for financial support, and Cluster Híbrido de Supercómputo Xiuhcoatl—CINVESTAV and Miztli—UNAM for computational resources. M.J. and J.T. acknowledge and CSC—IT Center for Science for computational resources (Project tty3979). M.J. also acknowledges the Finnish Doctoral Programme in Computational Sciences (FICS) for funding. J.T., M.J., T.R., and W.K. acknowledge the funding from the Academy of Finland (Centre of Excellence program) and the European Research Council (Advanced Grant project CROWDED-PRO-LIPIDS). W.K. acknowledges CSC—IT

DOI: 10.1021/acs.jpcb.5b04878
J. Phys. Chem. B 2015, 119, 15075−15088

Centre for Science (Espoo, Finland) for excellent computational resources (Project tty3995). M.S.M. acknowledges financial support from the Volkswagen Foundation (86110). L.M. acknowledges funding provided by the Institut National de la Santé et de la Recherche Médicale (INSERM). J.M. acknowledges CSC—IT Center for Science for computational resources. O.H.S.O. acknowledges Tiago Ferreira and Paavo Kinnunen for useful discussions, the Emil Aaltonen foundation for financial support, Aalto Science—IT project, and CSC—IT Center for Science for computational resources. H.S. acknowledges Catherine Etchebest and Stéphane Téletchéa for useful discussions and continued support, the HPC resources granted from GENCI-CINES (Grant 2014-c2014077209), and computer facilities provided by Région Ile de France and INTS (SESAME 2009 project).

REFERENCES

(1) *Structure and Dynamics of Membranes*; Lipowsky, R., Sackmann, E., Eds.; Elsevier: New York, 1995.
(2) Tieleman, D. P.; Marrink, S. J.; Berendsen, H. J. C. A computer perspective of membranes: molecular dynamics studies of lipid bilayer systems. *Biochim. Biophys. Acta, Rev. Biomembr.* **1997**, *1331*, 235−270.
(3) Klauda, J. B.; Venable, R. M.; MacKerell, A. D. Jr.; Pastor, R. W. In *Computational Modeling of Membrane Bilayers*; Feller, S. E., Ed.; Current Topics in Membranes; Academic Press: New York, 2008; Vol. *60*; pp 1−48.
(4) Edholm, O. In *Computational Modeling of Membrane Bilayers*; Feller, S. E., Ed.; Current Topics in Membranes; Academic Press: New York, 2008; Vol. *60*; pp 91−110.
(5) Tieleman, D. P. In *Molecular Simulations and Biomembranes: From Biophysics to Function*; Sansom, M., Biggin, P., Eds.; The Royal Society of Chemistry: London, 2010; pp 1−25.
(6) Piggot, T. J.; Piñeiro, Á; Khalid, S. Molecular Dynamics Simulations of Phosphatidylcholine Membranes: A Comparative Force Field Study. *J. Chem. Theory Comput.* **2012**, *8*, 4593−4609.
(7) Rabinovich, A.; Lyubartsev, A. Computer simulation of lipid membranes: Methodology and achievements. *Polym. Sci., Ser. C* **2013**, *55*, 162−180.
(8) Marsh, D. *Handbook of Lipid Bilayers*, 2nd ed.; RSC Press: London, 2013.
(9) Israelachvili, J. N.; Marcelja, S.; Horn, R. G. Physical Principles of Membrane Organization. *Q. Rev. Biophys.* **1980**, *13*, 121−200.
(10) Seelig, J.; Gally, H.-U.; Wohlgemuth, R. Orientation and flexibility of the choline head group in phosphatidylcholine bilayers. *Biochim. Biophys. Acta, Biomembr.* **1977**, *467*, 109−119.
(11) Skarjune, R.; Oldfield, E. Physical studies of cell surface and cell membrane structure. Determination of phospholipid head group organization by deuterium and phosphorus nuclear magnetic resonance spectroscopy. *Biochemistry* **1979**, *18*, 5903−5909.
(12) Jacobs, R. E.; Oldfield, E. NMR of membranes. *Prog. Nucl. Magn. Reson. Spectrosc.* **1980**, *14*, 113−136.
(13) Davis, J. H. The description of membrane lipid conformation, order and dynamics by 2H-NMR. *Biochim. Biophys. Acta, Rev. Biomembr.* **1983**, *737*, 117−171.
(14) Strenk, L.; Westerman, P.; Doane, J. A model of orientational ordering in phosphatidylcholine bilayers based on conformational analysis of the glycerol backbone region. *Biophys. J.* **1985**, *48*, 765−773.
(15) Akutsu, H.; Nagamori, T. Conformational analysis of the polar head group in phosphatidylcholine bilayers: a structural change induced by cations. *Biochemistry* **1991**, *30*, 4510−4516.
(16) Hong, M.; Schmidt-Rohr, K.; Nanz, D. Study of phospholipid structure by 1H, 13C, and 31P dipolar couplings from two-dimensional NMR. *Biophys. J.* **1995**, *69*, 1939−1950.
(17) Hong, M.; Schmidt-Rohr, K.; Zimmermann, H. Conformational Constraints on the Headgroup and sn-2 Chain of Bilayer DMPC from NMR Dipolar Couplings. *Biochemistry* **1996**, *35*, 8335−8341.
(18) Semchyschyn, D. J.; Macdonald, P. M. Conformational response of the phosphatidylcholine headgroup to bilayer surface charge: torsion angle constraints from dipolar and quadrupolar couplings in bicelles. *Magn. Reson. Chem.* **2004**, *42*, 89−104.
(19) Hauser, H.; Guyer, W.; Pascher, I.; Skrabal, P.; Sundell, S. Polar group conformation of phosphatidylcholine. Effect of solvent and aggregation. *Biochemistry* **1980**, *19*, 366−373.
(20) Hauser, H.; Guyer, W.; Paltauf, F. Polar group conformation of 1,2-di-O-alkylglycerophosphocholines in the absence and presence of ions. *Chem. Phys. Lipids* **1981**, *29*, 103−120.
(21) Hauser, H.; Pascher, I.; Pearson, R.; Sundell, S. Preferred conformation and molecular packing of phosphatidylethanolamine and phosphatidylcholine. *Biochim. Biophys. Acta, Rev. Biomembr.* **1981**, *650*, 21−51.
(22) Akutsu, H. Direct determination by Raman scattering of the conformation of the choline group in phospholipid bilayers. *Biochemistry* **1981**, *20*, 7359−7366.
(23) Pascher, I.; Lundmark, M.; Nyholm, P.-G.; Sundell, S. Crystal structures of membrane lipids. *Biochim. Biophys. Acta, Rev. Biomembr.* **1992**, *1113*, 339−373.
(24) Hauser, H.; Pascher, I.; Sundell, S. Preferred conformation and dynamics of the glycerol backbone in phospholipids. An NMR and x-ray single-crystal analysis. *Biochemistry* **1988**, *27*, 9166−9174.
(25) Marsh, D.; PÁli, T. Lipid conformation in crystalline bilayers and in crystals of transmembrane proteins. *Chem. Phys. Lipids* **2006**, *141*, 48−65.
(26) Gally, H. U.; Pluschke, G.; Overath, P.; Seelig, J. Structure of Escherichia coli membranes. Glycerol auxotrophs as a tool for the analysis of the phospholipid head-group region by deuterium magnetic resonance. *Biochemistry* **1981**, *20*, 1826−1831.
(27) Scherer, P.; Seelig, J. Structure and dynamics of the phosphatidylcholine and the phosphatidylethanolamine head group in L-M fibroblasts as studied by deuterium nuclear magnetic resonance. *EMBO J.* **1987**, *6*, 2915−2922.
(28) Shinoda, W.; Namiki, N.; Okazaki, S. Molecular dynamics study of a lipid bilayer: Convergence, structure, and long-time dynamics. *J. Chem. Phys.* **1997**, *106*, 5731−5743.
(29) Högberg, C.-J.; Nikitin, A. M.; Lyubartsev, A. P. Modification of the CHARMM force field for DMPC lipid bilayer. *J. Comput. Chem.* **2008**, *29*, 2359−2369.
(30) Castro, V.; Stevensson, B.; Dvinskikh, S. V.; Högberg, C.-J.; Lyubartsev, A. P.; Zimmermann, H.; Sandström, D.; Maliniak, A. NMR investigations of interactions between anesthetics and lipid bilayers. *Biochim. Biophys. Acta, Biomembr.* **2008**, *1778*, 2604−2611.
(31) Klauda, J. B.; Venable, R. M.; Freites, J. A.; O'Connor, J. W.; Tobias, D. J.; Mondragon-Ramirez, C.; Vorobyov, I.; MacKerrell, A. D., Jr; Pastor, R. W. Update of the CHARMM All-Atom Additive Force Field for Lipids: Validation on Six Lipid Types. *J. Phys. Chem. B* **2010**, *114*, 7830−7843.
(32) Kapla, J.; Stevensson, B.; Dahlberg, M.; Maliniak, A. Molecular Dynamics Simulations of Membranes Composed of Glycolipids and Phospholipids. *J. Phys. Chem. B* **2012**, *116*, 244−252.
(33) Dickson, C. J.; Rosso, L.; Betz, R. M.; Walker, R. C.; Gould, I. R. GAFFlipid: a General Amber Force Field for the accurate molecular dynamics simulation of phospholipid. *Soft Matter* **2012**, *8*, 9617−9627.
(34) Poger, D.; Mark, A. E. Lipid Bilayers: The Effect of Force Field on Ordering and Dynamics. *J. Chem. Theory Comput.* **2012**, *8*, 4807−4817.
(35) Ferreira, T. M.; Coreta-Gomes, F.; Ollila, O. H. S.; Moreno, M. J.; Vaz, W. L. C.; Topgaard, D. Cholesterol and POPC segmental order parameters in lipid membranes: solid state 1H-13C NMR and MD simulation studies. *Phys. Chem. Chem. Phys.* **2013**, *15*, 1976−1989.
(36) Chowdhary, J.; Harder, E.; Lopes, P. E. M.; Huang, L.; MacKerell, A. D.; Roux, B. A Polarizable Force Field of Dipalmitoylphosphatidylcholine Based on the Classical Drude Model for Molecular Dynamics Simulations of Lipids. *J. Phys. Chem. B* **2013**, *117*, 9142−9160.
(37) Maciejewski, A.; Pasenkiewicz-Gierula, M.; Cramariuc, O.; Vattulainen, I.; Rog, T. Refined OPLS All-Atom Force Field for Saturated Phosphatidylcholine Bilayers at Full Hydration. *J. Phys. Chem. B* **2014**, *118*, 4571−4581.

DOI: 10.1021/acs.jpcb.5b04878
J. Phys. Chem. B 2015, 119, 15075−15088

(38) Robinson, A.; Richards, W.; Thomas, P.; Hann, M. Head group and chain behavior in biological membranes: a molecular dynamics computer simulation. *Biophys. J.* **1994**, *67*, 2345−2354.
(39) Essex, J. W.; Hann, M. M.; Richards, W. G. Molecular Dynamics Simulation of a Hydrated Phospholipid Bilayer. *Philos. Trans. R. Soc., B* **1994**, *344*, 239−260.
(40) Kothekar, V. Molecular dynamics simulation of hydrated phospholipid bilayers. *Ind. J. Biochem. Biophys.* **1996**, *33*, 431−447.
(41) Hyvönen, M. T.; Rantala, T. T.; Ala-Korpela, M. Structure and Dynamic Properties of Diunsaturated 1-Palmitoyl-2-Linoleoyl-sn-Glycero-3-Phosphatidylcholine Lipid Bilayer from Molecular Dynamics Simulation. *Biophys. J.* **1997**, *73*, 2907−2923.
(42) Duong, T. H.; Mehler, E. L.; Weinstein, H. Molecular Dynamics Simulation of Membranes and a Transmembrane Helix. *J. Comput. Phys.* **1999**, *151*, 358−387.
(43) Prakash, P.; Sankararamakrishnan, R. Force field dependence of phospholipid headgroup and acyl chain properties: Comparative molecular dynamics simulations of DMPC bilayers. *J. Comput. Chem.* **2010**, *31*, 266−277.
(44) Berger, O.; Edholm, O.; Jähnig, F. Molecular dynamics simulations of a fluid bilayer of dipalmitoylphosphatidylcholine at full hydration, constant pressure, and constant temperature. *Biophys. J.* **1997**, *72*, 2002−2013.
(45) Bechinger, B.; Seelig, J. Conformational changes of the phosphatidylcholine headgroup due to membrane dehydration. A 2H-NMR study. *Chem. Phys. Lipids* **1991**, *58*, 1−5.
(46) Ulrich, A.; Watts, A. Molecular response of the lipid headgroup to bilayer hydration monitored by 2H-NMR. *Biophys. J.* **1994**, *66*, 1441−1449.
(47) Dvinskikh, S. V.; Castro, V.; Sandstrom, D. Probing segmental order in lipid bilayers at variable hydration levels by amplitude- and phase-modulated cross-polarization NMR. *Phys. Chem. Chem. Phys.* **2005**, *7*, 3255−3257.
(48) Brown, M. F.; Seelig, J. Influence of cholesterol on the polar region of phosphatidylcholine and phosphatidylethanolamine bilayers. *Biochemistry* **1978**, *17*, 381−384.
(49) Brown, M. F.; Seelig, J. Ion-induced changes in head group conformation of lecithin bilayers. *Nature* **1977**, *269*, 721−723.
(50) Akutsu, H.; Seelig, J. Interaction of metal ions with phosphatidylcholine bilayer membranes. *Biochemistry* **1981**, *20*, 7366−7373.
(51) Altenbach, C.; Seelig, J. Calcium binding to phosphatidylcholine bilayers as studied by deuterium magnetic resonance. Evidence for the formation of a calcium complex with two phospholipid molecules. *Biochemistry* **1984**, *23*, 3913−3920.
(52) Roux, M.; Bloom, M. Calcium, magnesium, lithium, sodium, and potassium distributions in the headgroup region of binary membranes of phosphatidylcholine and phosphatidylserine as seen by deuterium NMR. *Biochemistry* **1990**, *29*, 7077−7089.
(53) Roux, M.; Bloom, M. Calcium binding by phosphatidylserine headgroups. Deuterium NMR study. *Biophys. J.* **1991**, *60*, 38−44.
(54) Gally, H. U.; Niederberger, W.; Seelig, J. Conformation and motion of the choline head group in bilayers of dipalmitoyl-3-sn-phosphatidylcholine. *Biochemistry* **1975**, *14*, 3647−3652.
(55) Scherer, P. G.; Seelig, J. Electric charge effects on phospholipid headgroups. Phosphatidylcholine in mixtures with cationic and anionic amphiphiles. *Biochemistry* **1989**, *28*, 7720−7728.
(56) Browning, J. L.; Akutsu, H. Local anesthetics and divalent cations have the same effect on the headgroups of phosphatidylcholine and phosphatidylethanolamine. *Biochim. Biophys. Acta, Biomembr.* **1982**, *684*, 172−178.
(57) Kelusky, E. C.; Smith, I. C. The influence of local anesthetics on molecular organization in phosphatidylethanolamine membranes. *Mol. Pharmacol.* **1984**, *26*, 314−321.
(58) Roux, M.; Neumann, J. M.; Hodges, R. S.; Devaux, P. F.; Bloom, M. Conformational changes of phospholipid headgroups induced by a cationic integral membrane peptide as seen by deuterium magnetic resonance. *Biochemistry* **1989**, *28*, 2313−2321.
(59) Kuchinka, E.; Seelig, J. Interaction of melittin with phosphatidylcholine membranes. Binding isotherm and lipid head-group conformation. *Biochemistry* **1989**, *28*, 4216−4221.
(60) Catte, A.; Girych, M.; Javanainen, M.; Miettinen, M. S.; Monticelli, L.; Määttä, J.; Oganesyan, V. S.; Ollila, O. H. S. *Electrometer concept and binding of cations to phospholipid bilayers* **2015**, DOI: 10.5281/zenodo.32175.
(61) Miettinen, S. M.; Ollila, O. H. S.; Botan, A.; Catte, A.; Edholm, O.; Favela, F.; Ferreira, T.; Fuchs, P.; Girych, M.; et al. *NMRLipids project* **2015**, DOI: 10.6084/m9.figshare.1585017. The NMRLipids collaboration.
(62) Gowers, T.; Nielsen, M. Massively collaborative mathematics. *Nature* **2009**, *461*, 879−881.
(63) Ollila, O. H. S. Response of the hydrophilic part of lipid membranes to changing conditions - a critical comparison of simulations to experiments. 2013; http://arxiv.org/abs/1309.2131v1.
(64) Ollila, S.; Miettinen, S. M. *On credits* **2015**, DOI: 10.6084/m9.figshare.1577577. The NMRLipids collaboration.
(65) Botan, A.; Favela-Rosales, F.; Fuchs, P. F. J.; Javanainen, M.; Kanduč, M.; Kulig, W.; Lamberg, A.; Loison, C.; Lyubartsev, A.; Miettinen, M. S.; et al. *nmrlipids.blogspot.fi: Final submission to the J. Phys. Chem. B* **2015**, DOI: 10.5281/zenodo.32689.
(66) Seelig, J. Deuterium magnetic resonance: theory and application to lipid membranes. *Q. Rev. Biophys.* **1977**, *10*, 353−418.
(67) Hong, M.; Schmidt-Rohr, K.; Pines, A. NMR Measurement of Signs and Magnitudes of C-H Dipolar Couplings in Lecithin. *J. Am. Chem. Soc.* **1995**, *117*, 3310−3311.
(68) Gross, J. D.; Warschawski, D. E.; Griffin, R. G. Dipolar Recoupling in MAS NMR: A Probe for Segmental Order in Lipid Bilayers. *J. Am. Chem. Soc.* **1997**, *119*, 796−802.
(69) Dvinskikh, S. V.; Castro, V.; Sandstrom, D. Efficient solid-state NMR methods for measuring heteronuclear dipolar couplings in unoriented lipid membrane systems. *Phys. Chem. Chem. Phys.* **2005**, *7*, 607−613.
(70) Ollila, S.; Miettinen, S. M.; Vogel, A. *Accuracy of order parameter measurements* **2015**, DOI: 10.6084/m9.figshare.1577576. The NMRLipids collaboration.
(71) Ollila, S.; Fuchs, P.; Javanainen, M.; Lamberg, A. *On the signs of the order parameters* **2015**, DOI: 10.6084/m9.figshare.1577578. The NMRLipids collaboration.
(72) Engel, A. K.; Cowburn, D. The origin of multiple quadrupole couplings in the deuterium NMR spectra of the 2 chain of 1,2 dipalmitoyl-sn-glycero-3-phosphorylcholine. *FEBS Lett.* **1981**, *126*, 169−171.
(73) Vogel, A.; Feller, S. Headgroup Conformations of Phospholipids from Molecular Dynamics Simulation: Sampling Challenges and Comparison to Experiment. *J. Membr. Biol.* **2012**, *245*, 23−28.
(74) Ollila, S.; Hyvönen, M. T.; Vattulainen, I. Polyunsaturation in Lipid Membranes: Dynamic Properties and Lateral Pressure Profiles. *J. Phys. Chem. B* **2007**, *111*, 3139−3150.
(75) Ferreira, T. M.; Ollila, O. H. S.; Pigliapochi, R.; Dabkowska, A. P.; Topgaard, D. Model-free estimation of the effective correlation time for CH bond reorientation in amphiphilic bilayers: 1H13C solid-state NMR and MD simulations. *J. Chem. Phys.* **2015**, *142*, 044905.
(76) Hess, B.; Kutzner, C.; van der Spoel, D.; Lindahl, E. GROMACS 4: Algorithms for Highly Efficient, Load-Balanced, and Scalable Molecular Simulation. *J. Chem. Theory Comput.* **2008**, *4*, 435−447.
(77) Plimpton, S. Fast Parallel Algorithms for Short-Range Molecular Dynamics. *J. Comput. Phys.* **1995**, *117*, 1−19.
(78) Lyubartsev, A. P.; Laaksonen, A. M. DynaMix a scalable portable parallel MD simulation package for arbitrary molecular mixtures. *Comput. Phys. Commun.* **2000**, *128*, 565−589.
(79) Phillips, J. C.; Braun, R.; Wang, W.; Gumbart, J.; Tajkhorshid, E.; Villa, E.; Chipot, C.; Skeel, R. D.; Kalé, L.; Schulten, K. Scalable molecular dynamics with NAMD. *J. Comput. Chem.* **2005**, *26*, 1781−1802.
(80) Gurtovenko, A. A.; Patra, M.; Karttunen, M.; Vattulainen, I. Cationic DMPC/DMTAP Lipid Bilayers: Molecular Dynamics Study. *Biophys. J.* **2004**, *86*, 3461−3472.

DOI: 10.1021/acs.jpcb.5b04878
J. Phys. Chem. B 2015, 119, 15075−15088

(81) Miettinen, M. S. *Molecular dynamics simulation trajectory of a fully hydrated DMPC lipid bilayer* **2013**, DOI: 10.6084/m9.figshare.829642.
(82) Miettinen, M. S.; Gurtovenko, A. A.; Vattulainen, I.; Karttunen, M. Ion Dynamics in Cationic Lipid Bilayer Systems in Saline Solutions. *J. Phys. Chem. B* **2009**, *113*, 9226−9234.
(83) Marrink, S.-J.; Berger, O.; Tieleman, P.; Jähnig, F. Adhesion Forces of Lipids in a Phospholipid Membrane Studied by Molecular Dynamics Simulations. *Biophys. J.* **1998**, *74*, 931−943.
(84) Määttä, J. DPPC_Berger. 2015; DOI: 10.5281/zenodo.13934.
(85) Ollila, O. H. S.; Ferreira, T.; Topgaard, D. MD simulation trajectory and related files for POPC bilayer (Berger model delivered by Tieleman, Gromacs 4.5). 2014; DOI: 10.5281/zenodo.13279.
(86) Ollila, O. H. S.; Miettinen, M. MD simulation trajectory and related files for DPPC bilayer (CHARMM36, Gromacs 4.5). 2015; DOI: 10.5281/zenodo.15549.
(87) Ollila, O. H. S.; Miettinen, M. MD simulation trajectory and related files for POPC bilayer (CHARMM36, Gromacs 4.5). 2015; DOI: 10.5281/zenodo.13944.
(88) Santuz, H. MD simulation trajectory and related files for POPC bilayer (CHARMM36, Gromacs 4.5). 2015; DOI: 10.5281/zenodo.14066.
(89) Kulig, W.; Pasenkiewicz-Gierula, M.; Róg, T. Cis and Trans Unsaturated Phosphatidylcholine Bilayers: A Molecular Dynamics Simulation Study. *Chem. Phys. Lipids* **2016**, *195*, 12−20.
(90) Javanainen, M. POPC @ 310K, model by Maciejewski and Rog. 2014; DOI: 10.5281/zenodo.13497.
(91) Javanainen, M. POPC/Cholesterol @ 310K, 0, 10, 40, 50 and 60 mol-% cholesterol. Model by Maciejewski and Rog. 2015; DOI: 10.5281/zenodo.13877.
(92) Javanainen, M. POPC @ 310K, varying water-to-lipid ratio. Model by Maciejewski and Rog. 2014; DOI: 10.5281/zenodo.13498.
(93) Ollila, O. H. S.; Retegan, M. MD simulation trajectory and related files for DPPC bilayer (GAFFlipid, Gromacs 4.5). 2015; DOI: 10.5281/zenodo.15550.
(94) Ollila, O. H. S.; Retegan, M. MD simulation trajectory and related files for POPC bilayer (GAFFlipid, Gromacs 4.5). 2015; DOI: 10.5281/zenodo.13791.
(95) Dickson, C. J.; Madej, B. D.; Skjevik, g. A.; Betz, R. M.; Teigen, K.; Gould, I. R.; Walker, R. C. Lipid14: The Amber Lipid Force Field. *J. Chem. Theory Comput.* **2014**, *10*, 865−879.
(96) Ollila, O. H. S.; Retegan, M. MD simulation trajectory and related files for POPC bilayer (Lipid14, Gromacs 4.5). 2014; DOI: 10.5281/zenodo.12767.
(97) Poger, D.; Van Gunsteren, W. F.; Mark, A. E. A new force field for simulating phosphatidylcholine bilayers. *J. Comput. Chem.* **2010**, *31*, 1117−1125.
(98) Fuchs, P. F. MD simulation trajectory and related files for DPPC bilayer in full hydration (Poger GROMOS53A6_L, Gromacs 4.0.7, PME, traj 1). 2015; DOI: 10.5281/zenodo.14594.
(99) Fuchs, P. F. MD simulation trajectory and related files for DPPC bilayer in full hydration (Poger GROMOS53A6_L, Gromacs 4.0.7, PME, traj 2). 2015; DOI: 10.5281/zenodo.14595.
(100) Jämbeck, J. P. M.; Lyubartsev, A. P. Derivation and Systematic Validation of a Refined All-Atom Force Field for Phosphatidylcholine Lipids. *J. Phys. Chem. B* **2012**, *116*, 3164−3179.
(101) Määttä, J. DPPC_Slipids. 2014; DOI: 10.5281/zenodo.13287.
(102) Jämbeck, J. P. M.; Lyubartsev, A. P. An Extension and Further Validation of an All-Atomistic Force Field for Biological Membranes. *J. Chem. Theory Comput.* **2012**, *8*, 2938−2948.
(103) Javanainen, M. POPC @ 310K, Slipids force field. 2015; DOI: 10.5281/zenodo.13887.
(104) Kukol, A. Lipid Models for United-Atom Molecular Dynamics Simulations of Proteins. *J. Chem. Theory Comput.* **2009**, *5*, 615−626.
(105) Javanainen, M. POPC @ 298K, Model by Kukol. 2014; DOI: 10.5281/zenodo.13393.
(106) Chiu, S.-W.; Pandit, S. A.; Scott, H. L.; Jakobsson, E. An Improved United Atom Force Field for Simulation of Mixed Lipid Bilayers. *J. Phys. Chem. B* **2009**, *113*, 2748−2763.
(107) Ollila, O. H. S. MD simulation trajectory and related files for POPC bilayer (Chiu et al. Gromos version, Gromacs 4.5). 2015; DOI: 10.5281/zenodo.15548.
(108) Lyubartsev, A.; et al. MD simulation trajectory and related files for DMPC bilayer, Högberg. *J. Comput. Chem.* **2008**, *29*, 2359. 2015
(109) Rabinovich, A. L.; Lyubartsev, A. P. Bond orientation properties in lipid molecules of membranes: molecular dynamics simulations. *J. Phys.: Conf. Ser.* **2014**, *510*, 012022.
(110) Lyubartsev, A. MD simulation trajectory and related files for POPC bilayer, Högberg et al parameters. *J. Comput. Chem.* **2008**, *29*, 2359. 2015
(111) Ulmschneider, J. P.; Ulmschneider, M. B. United Atom Lipid Parameters for Combination with the Optimized Potentials for Liquid Simulations All-Atom Force Field. *J. Chem. Theory Comput.* **2009**, *5*, 1803−1813.
(112) Javanainen, M. POPC @ 310K, Model by Ulmschneider and Ulmschneider. 2014; DOI: 10.5281/zenodo.13392.
(113) Tjörnhammar, R.; Edholm, O. Reparameterized United Atom Model for Molecular Dynamics Simulations of Gel and Fluid Phosphatidylcholine Bilayers. *J. Chem. Theory Comput.* **2014**, *10*, 5706−5715.
(114) Javanainen, M. DPPC @ 323K, new FF by Tjörnhammar and Edholm. 2014; DOI: 10.5281/zenodo.12743.
(115) Henin, J.; Shinoda, W.; Klein, M. L. United-Atom Acyl Chains for CHARMM Phospholipids. *J. Phys. Chem. B* **2008**, *112*, 7008−7015.
(116) Botan, A. DLPC @ 323K, CHARMM36UA force field. 2015; DOI: 10.5281/zenodo.13821.
(117) Lee, S.; Tran, A.; Allsopp, M.; Lim, J. B.; Henin, J.; Klauda, J. B. CHARMM36 United Atom Chain Model for Lipids and Surfactants. *J. Phys. Chem. B* **2014**, *118*, 547−556.
(118) Loison, C. Hydrated DPPC, MD simulation trajectory and related files for UA charmm36 model by Lee et al 2014. 2015; DOI: 10.5281/zenodo.17004.
(119) Ollila, O. H. S. MD simulation trajectory and related files for POPC bilayer in low hydration (Berger model delivered by Tieleman, Gromacs 4.5). 2015; DOI: 10.5281/zenodo.13814.
(120) Kanduč, M.; Schneck, E.; Netz, R. R. Hydration Interaction between Phospholipid Membranes: Insight into Different Measurement Ensembles from Atomistic Molecular Dynamics Simulations. *Langmuir* **2013**, *29*, 9126−9137.
(121) Kanduc, M. MD trajectory for DLPC bilayer (Berger, Gromacs 4.5.4), nw/28 w/l. 2015; DOI: 10.5281/zenodo.16287.
(122) Kanduc, M. MD trajectory for DLPC bilayer (Berger, Gromacs 4.5.4), nw/24 w/l. 2015; DOI: 10.5281/zenodo.16289.
(123) Kanduc, M. MD trajectory for DLPC bilayer (Berger, Gromacs 4.5.4), nw/20 w/l. 2015; DOI: 10.5281/zenodo.16291.
(124) Kanduc, M. MD trajectory for DLPC bilayer (Berger, Gromacs 4.5.4), nw/16 w/l. 2015; DOI: 10.5281/zenodo.16292.
(125) Kanduc, M. MD trajectory for DLPC bilayer (Berger, Gromacs 4.5.4), nw/12 w/l. 2015; DOI: 10.5281/zenodo.16293.
(126) Kanduc, M. MD trajectory for DLPC bilayer (Berger, Gromacs 4.5.4), nw/8 w/l. 2015; DOI: 10.5281/zenodo.16294.
(127) Kanduc, M. MD trajectory for DLPC bilayer (Berger, Gromacs 4.5.4), nw/4 w/l. 2015; DOI: 10.5281/zenodo.16295.
(128) Ollila, O. H. S.; Miettinen, M. MD simulation trajectory and related files for POPC bilayer in medium low hydration (CHARMM36, Gromacs 4.5). 2015; DOI: 10.5281/zenodo.13946.
(129) Ollila, O. H. S.; Miettinen, M. MD simulation trajectory and related files for POPC bilayer in low hydration (CHARMM36, Gromacs 4.5). 2015; DOI: 10.5281/zenodo.13945.
(130) Ollila, O. H. S. MD simulation trajectory and related files for POPC bilayer in low hydration (GAFFlipid, Gromacs 4.5). 2015; DOI: 10.5281/zenodo.13853.
(131) Höltje, M.; Förster, T.; Brandt, B.; Engels, T.; von Rybinski, W.; Höltje, H.-D. Molecular dynamics simulations of stratum corneum lipid models: fatty acids and cholesterol. *Biochim. Biophys. Acta, Biomembr.* **2001**, *1511*, 156−167.
(132) Ollila, O. H. S.; Ferreira, T.; Topgaard, D. MD simulation trajectory and related files for POPC/cholesterol (7 mol%) bilayer

DOI: 10.1021/acs.jpcb.5b04878
J. Phys. Chem. B 2015, 119, 15075−15088

(Berger model delivered by Tieleman, modified Höltje, Gromacs 4.5). 2014; DOI: 10.5281/zenodo.13282.
(133) Ollila, O. H. S.; Ferreira, T.; Topgaard, D. MD simulation trajectory and related files for POPC/cholesterol (15 mol%) bilayer (Berger model delivered by Tieleman, modified Höltje, Gromacs 4.5). 2014; DOI: 10.5281/zenodo.13281.
(134) Ollila, O. H. S.; Ferreira, T.; Topgaard, D. *MD simulation trajectory and related files for POPC/cholesterol (34 mol%) bilayer (Berger model delivered by Tieleman, modified Höltje, Gromacs 4.5)*. 2014; DOI: 10.5281/zenodo.13283.
(135) Ollila, O. H. S.; Ferreira, T.; Topgaard, D. MD simulation trajectory and related files for POPC/cholesterol (50 mol%) bilayer (Berger model delivered by Tieleman, modified Höltje, Gromacs 4.5). 2014; DOI: 10.5281/zenodo.13285.
(136) Ollila, O. H. S.; Ferreira, T.; Topgaard, D. MD simulation trajectory and related files for POPC/cholesterol (60 mol%) bilayer (Berger model delivered by Tieleman, modified Höltje, Gromacs 4.5). 2014; DOI: 10.5281/zenodo.13286.
(137) Lim, J. B.; Rogaski, B.; Klauda, J. B. Update of the Cholesterol Force Field Parameters in CHARMM. *J. Phys. Chem. B* **2012**, *116*, 203−210.
(138) Favela-Rosales, F. POPC_Glycerol_CHARMM36_0−10−15−20−25−35−50%CHOL. 2015; DOI: 10.5281/zenodo.16830.
(139) Santuz, H. MD simulation trajectory for POPC/20% Chol bilayer (CHARMM36, Gromacs 4.5). 2015; DOI: 10.5281/zenodo.14067.
(140) Santuz, H. MD simulation trajectory for POP @ C/50% Chol bilayer (CHARMM36, Gromacs 4.5). 2015; DOI: 10.5281/zenodo.14068.
(141) Warschawski, D.; Devaux, P. Order parameters of unsaturated phospholipids in membranes and the effect of cholesterol: a 1H-13C solid-state NMR study at natural abundance. *Eur. Biophys. J.* **2005**, *34*, 987−996.
(142) Mashl, R. J.; Scott, H. L.; Subramaniam, S.; Jakobsson, E. Molecular Simulation of Dioleoylphosphatidylcholine Lipid Bilayers at Differing Levels of Hydration. *Biophys. J.* **2001**, *81*, 3005−3015.
(143) Pertsin, A.; Platonov, D.; Grunze, M. Direct computer simulation of water-mediated force between supported phospholipid membranes. *J. Chem. Phys.* **2005**, *122*, 244708.
(144) Pertsin, A.; Platonov, D.; Grunze, M. Origin of Short-Range Repulsion between Hydrated Phospholipid Bilayers:? A Computer Simulation Study. *Langmuir* **2007**, *23*, 1388−1393.
(145) Eun, C.; Berkowitz, M. L. Origin of the Hydration Force: Water-Mediated Interaction between Two Hydrophilic Plates. *J. Phys. Chem. B* **2009**, *113*, 13222−13228.
(146) Eun, C.; Berkowitz, M. L. Thermodynamic and Hydrogen-Bonding Analyses of the Interaction between Model Lipid Bilayers. *J. Phys. Chem. B* **2010**, *114*, 3013−3019.
(147) Schneck, E.; Sedlmeier, F.; Netz, R. R. Hydration repulsion between biomembranes results from an interplay of dehydration and depolarization. *Proc. Natl. Acad. Sci. U. S. A.* **2012**, *109*, 14405−14409.
(148) Israelachvili, J. N. *Intermolecular and Surface Forces*; Academic Press: London, 1985.
(149) Israelachvili, J. N.; Wennerström, H. Role of hydration and water structure in biological and colloidal interactions. *Nature* **1996**, *379*, 219−225.
(150) Sparr, E.; Wennerström, H. Interlamellar forces and the thermodynamic characterization of lamellar phospholipid systems. *Curr. Opin. Colloid Interface Sci.* **2011**, *16*, 561−567.
(151) Simons, K.; Vaz, W. L. Model Systems, Lipid Rafts, And Cell Membranes. *Annu. Rev. Biophys. Biomol. Struct.* **2004**, *33*, 269−295.
(152) Somerharju, P.; Virtanen, J. A.; Cheng, K. H.; Hermansson, M. The superlattice model of lateral organization of membranes and its implications on membrane lipid homeostasis. *Biochim. Biophys. Acta, Biomembr.* **2009**, *1788*, 12−23.
(153) Huang, J.; Feigenson, G. W. A Microscopic Interaction Model of Maximum Solubility of Cholesterol in Lipid Bilayers. *Biophys. J.* **1999**, *76*, 2142−2157.
(154) Zhu, Q.; Cheng, K. H.; Vaughn, M. W. Molecular Dynamics Studies of the Molecular Structure and Interactions of Cholesterol Superlattices and Random Domains in an Unsaturated Phosphatidylcholine Bilayer Membrane. *J. Phys. Chem. B* **2007**, *111*, 11021−11031.
(155) Róg, T.; Pasenkiewicz-Gierula, M.; Vattulainen, I.; Karttunen, M. Ordering effects of cholesterol and its analogues. *Biochim. Biophys. Acta, Biomembr.* **2009**, *1788*, 97−121.
(156) Alwarawrah, M.; Dai, J.; Huang, J. Modification of Lipid Bilayer Structure by Diacylglycerol: A Comparative Study of Diacylglycerol and Cholesterol. *J. Chem. Theory Comput.* **2012**, *8*, 749−758.
(157) Marsh, D. Liquid-ordered phases induced by cholesterol: A compendium of binary phase diagrams. *Biochim. Biophys. Acta, Biomembr.* **2010**, *1798*, 688−699.
(158) Ghosh, R.; Seelig, J. The interaction of cholesterol with bilayers of phosphatidylethanolamine. *Biochim. Biophys. Acta, Biomembr.* **1982**, *691*, 151−160.
(159) Ferreira, T. M.; Topgaard, D.; Ollila, O. H. S. Molecular Conformation and Bilayer Pores in a Nonionic Surfactant Lamellar Phase Studied with 1H13C Solid-State NMR and Molecular Dynamics Simulations. *Langmuir* **2014**, *30*, 461−469.

DOI: 10.1021/acs.jpcb.5b04878
J. Phys. Chem. B 2015, 119, 15075−15088